

# Lab Report

## S261: Optical Astronomy and Gravitational Lensing

Chenhuan Wang and Harilal Bhattarai

September 11, 2020

### 1 Background<sup>1</sup>

#### 1.1 Cosmic Expansion

A spatially homogeneous and isotropic Universe can be described as FLRW metric. Solving Einstein's field equations with FLRW metric gives expansion of the Universe [2]. Hubble parameter  $H(t) = \dot{a}(t)/a(t)$  evolves according to

$$H^2(t) = H_0^2 [\Omega_{\text{rad}} a^{-4}(t) + \Omega_{\text{mat}} a^{-3}(t) + \Omega_{\text{curv}} a^{-2}(t) + \Omega_{\Lambda}] \quad (1)$$

Because of expansion of the Universe, light emitted in the past gets redshifted over time. The redshift of a source is given by,

$$z = \frac{\lambda_{\text{obj}} - \lambda_{\text{em}}}{\lambda_{\text{em}}} \quad (2)$$

Where,  $\lambda_{\text{obs}}$  and  $\lambda_{\text{em}}$  are, respectively, the wavelengths at time of observation and emission. Redshift is directly related to the scale factor by,

$$1 + z = \frac{1}{a(t_{\text{em}})} \quad (3)$$

with scale factor at present time defined as  $a(t_0) = 1$ .

The local Hubble law are given by the following formula,

$$v_{\text{esc}} = H_0 D \quad (4)$$

where,  $H_0 = H(t_0)$  is Hubble constant and  $D$  is the distance between object and observer.

---

<sup>1</sup>Content taken from [1], if not noted otherwise.

## 1.2 Distances

Accordingly, one defines the angular diameter distance as exactly this ratio,

$$D_{\text{ang}}(z) = 2R/\delta = a(z)f_K(w) \quad (5)$$

Where,  $R$  is the radius of the distant object,  $\delta$  is the angular diameter, and  $z$  is the cosmological redshift. If we consider an observer at redshift  $z_1$  gives the angular diameter of another object at redshift  $z_2$ , so equation 5 becomes

$$D_{\text{ang}}(z_1, z_2) = a(z_2)f_K[w(z_2) - w(z_1)] \quad (6)$$

Another distance measure relates the observed flux,  $S$ , of a source to its luminosity,  $L$ . For a known luminosity, the distance to the source can be determined as,

$$D_{\text{lum}}(z) = \sqrt{\frac{L}{4\pi S}} \quad (7)$$

## 1.3 Quasars

## 1.4 Gravitational lensing

Figure 1: Schematic diagram of the gravitational lensing system [\[wiki\]](#). [picture and citation missing!](#)

### 1.4.1 Lens Equation

For simplicity, we assume that all angles considers are small so that  $\tan x \approx \sin x \approx x$ , source plane and lens plane are parallel, and light travels in straight line in between planes. For a given source, the lens equation is given by,

$$\boldsymbol{\beta} = \boldsymbol{\theta} - \boldsymbol{\alpha}(\boldsymbol{\theta}) \quad (8)$$

where,  $\boldsymbol{\theta}$  is the apparent angular position of the source in the sky,  $\boldsymbol{\beta}$  is its true position, and  $\boldsymbol{\alpha}$  is the scaled deflection angle.

Now, we can define a dimensionless surface mass density with convergence as,

$$\kappa(\boldsymbol{\theta}) = \frac{\sum(D_d\boldsymbol{\theta})}{\sum_{\text{cr}}} \quad (9)$$

with the critical surface mass density,

$$\Sigma_{\text{cr}} = \frac{c^2}{4\pi G} \frac{D_s}{D_d D_{ds}} \quad (10)$$

The scaled deflection angle can be rewritten as,

$$\boldsymbol{\alpha}(\boldsymbol{\theta}) = \frac{1}{\pi} \int d^2\theta' \kappa(\boldsymbol{\theta}') \frac{\boldsymbol{\theta} - \boldsymbol{\theta}'}{|\boldsymbol{\theta} - \boldsymbol{\theta}'|^2} \quad (11)$$

For further convenience, a deflection potential is introduced

$$\psi(\boldsymbol{\theta}) = \frac{1}{\pi} \int d^2\theta' \kappa(\boldsymbol{\theta}') \ln |\boldsymbol{\theta} - \boldsymbol{\theta}'| \quad (12)$$

The use of this quantity is well-motivated because it encloses all information of the mass distribution of the lens [1]. In addition, relation of deflection potential and deflection angle can be found

$$\boldsymbol{\alpha}(\boldsymbol{\theta}) = \nabla\psi(\boldsymbol{\theta}) \quad (13)$$

From the deflection potential a further scalar function, the Fermat potential, can be defined

$$\tau(\boldsymbol{\theta}; \boldsymbol{\beta}) = \frac{1}{2}(\boldsymbol{\beta} - \boldsymbol{\theta})^2 - \psi(\boldsymbol{\theta}) \quad (14)$$

Finally to find the magnification of the images is given by

$$\mu = (\det A)^{-1} \quad (15)$$

where, A is the Jacobian matrix of lens mapping.

$$A_{ij} = \frac{\partial\beta_i}{\partial\theta_j} \quad (16)$$

#### 1.4.2 The SIS (Singular Isothermal Sphere)

A simple model to describe the mass distribution of a galaxy acting as a lens is the singular isothermal sphere (SIS):

$$\rho(r) = \frac{\sigma_v^2}{2\pi G r^2} \quad (17)$$

where  $\sigma_v$  is the velocity dispersion. Physically this means that the lens system consists of self-gravitating with Maxwellian velocity distribution [3].

Integration along the line of sight yields the surface mass density

$$\Sigma(\xi) = \frac{\sigma_v^2}{2G\xi} \quad (18)$$

A characteristic angular scale of an axisymmetric lens is given by the Einstein radius  $\theta_E$ , defined as the angle inside which the mean of the convergence is unity. As a consequence, the projected mass inside  $\theta_E$  can be written as,

$$M(\theta \leq \theta_E) = \pi\theta_E^2 D_d^2 \Sigma_{cr} \quad (19)$$

For an SIS the Einstein radius reads

$$\theta_E = 4\pi \left( \frac{\sigma_v}{c} \right)^2 \frac{D_{ds}}{D_s} \quad (20)$$

## 1.5 Calibration frames

## 1.6 Image reduction

# 2 Preparatory Tasks

### P.3.1 Calculation of the deflection potential, $\psi(\theta)$ and the scaled deflection angle of an SIS lens.

From equation 12 the deflection potential, which gives the information about the mass distribution of the lens, is define as,

$$\psi(\theta) = \frac{1}{\pi} \int d^2\theta' \kappa(\theta') \ln |\theta - \theta'| \quad (21)$$

In the case of axial symmetry of SIS lens equation 12 simplifies to (Given on the question)

$$\psi(\theta) = 2 \int_0^\theta d\theta' \theta' \kappa(\theta') \ln\left(\frac{\theta}{\theta'}\right) \quad (22)$$

By substituting the values of  $\Sigma(D_d\theta)$ , where  $D_d\theta = \xi$  from equation 18 and  $\Sigma_{cr}$  from equation 10 on equation 9, then by plugging the new expression of  $\kappa(\theta)$  equation 22 becomes

$$\psi(\theta) = \frac{4\pi}{c^2} \frac{D_{ds}}{D_s} \sigma_v^2 \int_0^\theta d\theta' \ln\left(\frac{\theta}{\theta'}\right) \quad (23)$$

By integrating,

$$= \frac{4\pi}{c^2} \frac{D_{ds}}{D_s} \sigma_v^2 [\theta' \ln\left(\frac{\theta}{\theta'}\right) + \theta'] \quad (24)$$

$$= \theta_E (\theta \ln \theta - \theta \ln \theta + \theta) \quad (25)$$

Therefore,

$$\psi(\theta) = \theta_E \theta \quad (26)$$

From equation 13 scaled deflection angle is defined as

$$\alpha(\theta) = \nabla \psi(\theta) \quad (27)$$

From equations: 26 and 27,

$$\alpha(\theta) = \nabla \theta_E \theta = \theta_E \hat{\theta} \quad (28)$$

### P.3.2: Solving the lens equation and finding the separation between images

The lens equation is given by,

$$\beta = \theta - \alpha(\theta) \quad (29)$$

By using the expression for scaled deflection angle for SIS from 28

$$\beta = \theta - \theta_E \hat{\theta} \quad (30)$$

or,

$$\alpha(\theta) = \beta + \theta_E \hat{\theta} \quad (31)$$

for  $\hat{\theta} > 0$ ,

$$\theta_A = \beta + \theta_E \quad (32)$$

for  $\hat{\theta} < 0$ ,

$$\theta_B = \beta - \theta_E \quad (33)$$

Thus, the separation of these images is given by,

$$\Delta\theta = \theta_A - \theta_B = \beta + \theta_E - (\beta - \theta_E) = 2\theta_E \quad (34)$$

### P.3.3: Magnification ratio of the two images of SIS lens.

The magnification of a gravitational lens is given by,

$$\mu = (\det A)^{-1} \quad (35)$$

### P.3.4: Time delay derivation for SIS lens as a function of $\theta_A$ and $\theta_B$ .

The time delay is given by[1]

$$c\Delta t(\beta) = (1 + z_d) \frac{D_d D_s}{D_{ds}} [\tau(\theta_A; \beta) - \tau(\theta_B; \beta)] \quad (36)$$

Also, from 14 the Format's potential is defined as,

$$\tau(\theta; \beta) = \frac{1}{2}(\beta - \alpha)^2 - \psi(\theta) \quad (37)$$

So,

$$\tau(\theta_A; \beta) = \frac{1}{2}(\beta - \theta_A)^2 - \psi(\theta_A) \quad (38)$$

By plugging the values of  $\beta$  and  $\psi(\theta_A)$ ,

$$= \frac{1}{2}(\theta_A - \theta_E - \theta_A)^2 - \theta_E \theta_A \quad (39)$$

Therefore,

$$\tau(\theta_A; \beta) = \frac{1}{2}\theta_E^2 - \theta_E \theta_A \quad (40)$$

Similarly,

$$\tau(\theta_B; \beta) = \frac{1}{2}(\beta - \theta_B)^2 - \psi(\theta_B) \quad (41)$$

$$= \frac{1}{2}(\theta_B + \theta_E - \theta_B)^2 - \theta_E \theta_B \quad (42)$$

$$\tau(\theta_B; \beta) = \frac{1}{2}\theta_E^2 - \theta_E\theta_B \quad (43)$$

By substituting these values equation 36 becomes,

$$c\Delta t(\beta) = (1 + z_d) \frac{D_d D_s}{D_{ds}} \left( \frac{1}{2}\theta_E^2 - \theta_E\theta_A - \frac{1}{2}\theta_E^2 + \theta_E\theta_B \right) \quad (44)$$

Therefore,

$$\Delta t(\beta) = \frac{(1 + z_d)}{c} \frac{D_d D_s}{D_{ds}} \theta_E (\theta_B - \theta_A) \quad (45)$$

Thus, the time delay is proportional to the Einstein radius.

### P3.5: Minimum Dispersion Estimator

The minimum dispersion estimator is a simple, efficient and well tested method to estimate time delay from observed light curve[1] It helps to find the difference between the curve at various delay times. Since it assumes that light curves have the same shape but they are separated by time.

### P3.6: The approximation of dispersion function near the minimum by a parabola.

The dispersion function near the minimum can be found by Taylor expanding of the functional function. i.e.

$$d^2(\lambda) = D^2(\lambda_0) + \frac{dD^2(\lambda_0)}{d\lambda}(\lambda - \lambda_0) + \frac{d^2D^2(\lambda_0)}{d\lambda^2}(\lambda - \lambda_0)^2 + 0 \quad (46)$$

Where,  $D^2$  is the dispersion function and  $\lambda$  is the time shift. Here high order terms are negligible compared to first and second order terms.

The dispersion function is minimum at  $\lambda = \lambda_0$ . Now the second term of equation 46 goes to zero. i.e.

$$d^2(\lambda) = D^2(\lambda_0) + \frac{d^2D^2(\lambda_0)}{d\lambda^2}(\lambda - \lambda_0)^2 \quad (47)$$

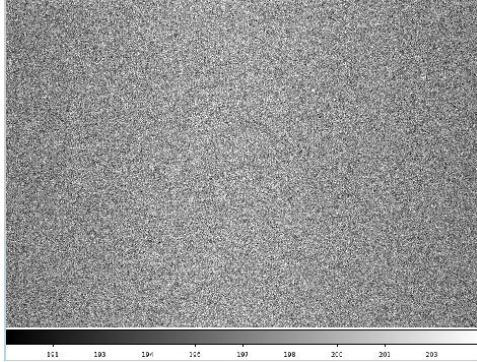
it is parabolic in shape.

### 3 Image reduction

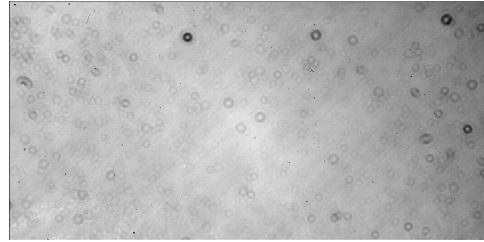
Calibration frames and science frames have been already taken. Dark frames are not provided and not necessary, since dark currents can be neglected in this case due to proper cooling. Here these images will get inspected and reduced as explained before.

#### 3.1 Raw-image inspection

Calibration images are firstly visually inspected using `ds9` with `zscale` setting. Figure 2a and 2b are examples of bias and flat frames. Note that images shown here are not the whole images.



(a) Bias frame



(b) Flat frame. Color legend was unfortunately not included in screenshot.

Figure 2: Calibration frames. Shown images are only central part of whole images.

Average bias level is somewhat near 200. This values changes, though not so obvious in figure 2a, throughout the image. Left and right sides are significantly darker, meaning less bias. Presumably it is related to geometry and layout of CCD chip. Sometimes one can see quite large white dots in bias picture. Positions of these white dots vary from image to image. Because of its significant size comparing to other noises, they are mostly likely to be cosmic rays, as hinted by [1].

Middle of bias frame is chosen to calculated background and sigma, due to its lack of large-scale variation. Output of `imstats` gives us mean and sigma:  $198.72 \pm 2.59$ . Noise here should be readout variations and random fluctuations [1].

In flat-field, most obvious feature is black circles or doughnuts. These are dusts on dewar windows and/or filter [1]. This results in lower photon counts, thus black in flat-field images. They are not on CCD chips, since they are not properly focused. Some large-scale structure can be seen. It can be explained by different quantum efficiency at different area of CCD. There are quite a lot small sharp black dots visibly. They are most likely to be bad pixels and dust directly on CCD chip.

Each flat-field has different exposure time. One can try to find correlation between mean value of image and exposure time using commands provided in [1]. Ratios between these two goes down with increasing exposure time. Firstly of all, CCD chips should be saturated here, since with exposure time, mean values goes down. One possibility is that read-out noise in circuit gets averaged out with long exposure time, thus lower ratio.

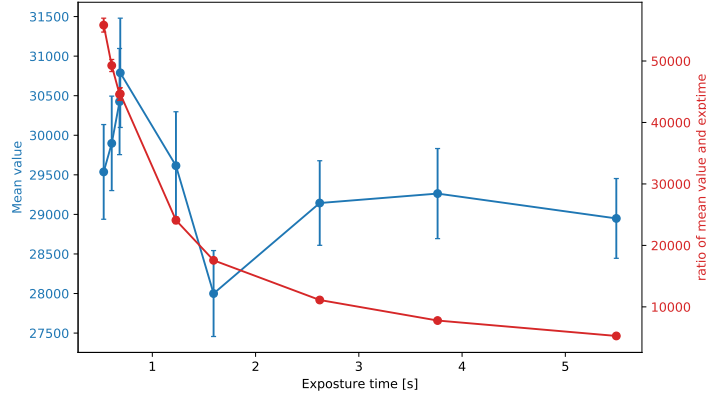


Figure 3: Mean values (red) with sigmas and the ratios (blue) against exposure time of flat-field images.

In science frame one can clearly see doughnut structures and sharp black dots as in flat-field frames. Between exposure, most out-standing change would be that telescope is moving around.

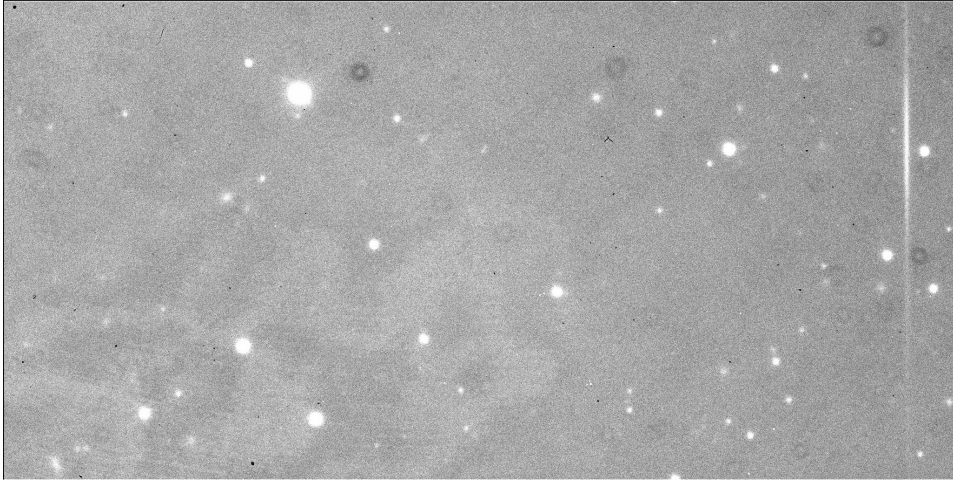


Figure 4: An example of science frame.

We use `image008068.fits` as an example and compute mean and sigma in area without bright objects. Values are  $693.20 \pm 19.00$ . It is greater than the mean value of bias frame. This is easy to understand, since science frame must contain sky.

### 3.2 Image reduction

Several science frames containing source `SDSS1650+4251` are taken from one filter ( $R$ ). Now these images will be reduced with help of calibration frames and some more in `theli`. `theli` mainly consists of several tabs or processing groups. Each of following paragraph corresponds one processing group/



**Initialise** First off, `theli` should be properly reset and initialised. Number of CPU cores and instrument (telescope) are specified accordingly. Paths containing bias, flat, and science frames are filled in.

**Preparation** Through this processing group, headers contained in `.fits` files can be split and/or corrected. Comparison of headers before and after corrections reveals

- size in  $x$  and  $y$  are swapped, meaning orientation of images has been changed,
- (useless) information, e.g. comments, CCD info, Date, and etc., has been removed,
- lots of lines starting with `DUMMY` have been added.

There are more changes, but the listed alterations are most noticeable.

**Calibration** In this step, calibration frames are getting co-added. In co-addition process, images are stacked on top of each other, while making sure each object falls onto the same pixel [1]. By doing this and in the end only calibrating with co-added images, random noises will get averaged out.

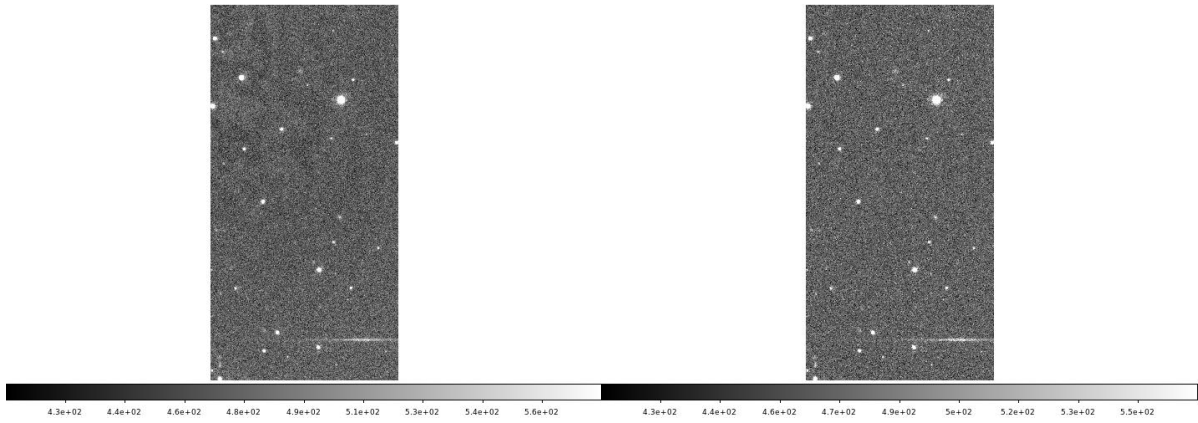
After co-addition, bias frames are free of small white dots as seen before and flat frames get a bit brighter. One can further compare noise dispersion of co-added bias frame and single bias frame. They are respectively 0.72 and 2.27. So noise level in co-added images is much lower.

The minimal value in normalised flat-field is 0. Dithering during co-addition helps to remove bright objects (stars and etc.).

**Background modelling** In this processing group, only background model correction is selected, where a superflat and fringe model is created and applied. Its configurations are set according to [1]: `DT = 1.0`, `DMIN = 10`, `mask expansion factor = 3`, `median combination, divide smoothed model, subtract fringes` method, smoothing kernel for background model = 256.

In superflat, one can clearly see fringes pattern. Fringes and background sky can be extracted with smoothing process. In `SDSS1650+4251_R_block0_1_fringe.fits`, there is only fringes visible and in `SDSS1650+4251_R_block0_1_illum.fits` only smooth gradient, i.e. background.

Correction given by illumination is roughly 500 (counts). Fringes are removed after correction, see figure 5a and 5b.



(a) Before correction. Pay attention to top left corner. (b) After correction. Pay attention to top left corner.

**Weighting** In this step, weighting and masking are performed to compensate bad pixels and different quantum efficiency. Global weights and WEIGHTS are created and applied.

#### **Astrometry/Photometry**

#### **Co-addition**

#### **4 PSF extraction**

#### **5 Component fitting**

#### **6 Time-delay estimate**

#### **7 Lensing analysis**

## References

- [1] Unknown. *Advanced lab course in physics at Bonn University: Optical Astronomy and Gravitational Lensing*. 2020.
- [2] Edward W. Kolb and Michael S. Turner. *The Early Universe*. Addison-Wesley, 1993.
- [3] P. Schneider. *Introduction to Gravitational Lensing and Cosmology*.